The University of South Bohemia in České Budějovice
Faculty of Science

Elucidation of the function of Kap60 and Kap95 in the tRNA retrograde pathway in *Trypanosoma brucei*

Bachelor thesis

Nina Dudáková

Supervisor: RNDr. Zdeněk Paris, PhD

České Budějovice 2024

Dudáková, N., 2024: Elucidation of the function of Kap60 and Kap95 in the tRNA retrograde pathway in *Trypanosoma brucei*. Bc. Thesis, in English - 42 p., Faculty of Science, University of South Bohemia, České Budějovice, Czech Republic.

Annotation

The aim of this thesis was to elucidate the role of Kap60 and Kap95 on tRNA retrograde pathway in procyclic form of *Trypanosoma brucei*.

Declaration

I declare that I am the author of this qualification thesis and that in writing it I have used the sources and literature displayed in the list of used sources only.

České Budějovice 09.05.2024 _____

Nina Dudáková

Acknowledgements

Firstly, I would like to express my deepest gratitude to my supervisor and PI, RNDr. Zdeněk Paris, PhD, for giving me the opportunity to complete my bachelor's thesis in his laboratory. I am grateful to Parda for guiding me through the complex world of tRNAs, for his support, and for his help with my professional development.

Moreover, I would like to thank PhD. Eva Hegedüsová for teaching me the necessary techniques and helping me with the basis of this thesis. Additionally, I would like to thank Eva for her never-ending patience and trust, which further enabled me to be independent in my work.

Lastly, I would like to extend my gratitude to all current and previous members of Parda's lab that I have had the privilege to meet: Eva M., Bankatesh, Sneha Veru, and Julie, for always helping me out when I needed them and for consistently maintaining a positive work attitude. I am grateful to have had my first lab experience in such a friendly atmosphere, which only further inspires me to work in science.

Abbreviations

aa	Amino acid
APS	Ammonium persulfate
Bp	Base pairs
DAPI	4′,6-diamino-2-phenylindole dihydrochloride
DNA	Deoxyribonucleic acid
dNTP	Deoxynucleotide triphosphate
E.coli	*Escherichia coli*
EtBr	Ethidium bromide
EtOH	Ethanol
FBS	Foetal bovine serum
GDP	Guanosine diphosphate
GTP	Guanosine triphosphate
Glu	Glutamic acid
IAA	Isoamyl alcohol
kDa	Kilodalton
LB	Lysogeny broth
mRNA	Messenger RNA
$NaIO_4$	Sodium periodate
NaOAc	Sodium acetate
NLS	Nuclear localisation signal
NPC	Nuclear pore complex
NTF	Nuclear transport factor
PBS	Phosphate buffered saline
PCR	Polymerase chain reaction

PF	Procyclic form
PNK	Poly nucleotide kinase
pre-tRNA	Precursor transfer RNA
RNA	Ribonucleic acid
RNAi	RNA interference
rpm	Rounds per minute
rRNA	Ribosomal RNA
SOC	Super optimal broth
TAE	Tris-acetate-EDTA
T. brucei	Trypanosoma brucei
Tet	Tetracycline
TEMED	Tetramethylethylenediamine
tRNA	Transfer RNA
Tyr	Tyrosine
UV	Ultraviolet

Table of Contents

1. Introduction

1.1. Transfer RNA

Translation is a complex biological process of mRNA decoding and subsequent synthesis of new polypeptide chains. During translation, the mRNA previously formed during transcription serves as a template for the formation of the polypeptide chains (Ibba & Söll, 1999).

Transfer ribonucleic acids (tRNAs) are 73-90 nucleotide-long molecules serving an integral part in this protein biosynthesis machinery. Following transcription, tRNAs are exported into the cytoplasm, where they become adaptor molecules responsible for the incorporation of amino acids into a newly synthesized polypeptide chain (Raina et al., 2014).

In addition to their primary role in protein biosynthesis, tRNAs are involved in numerous biological processes. These include monitoring of nutritional stress, signalling, and apoptosis control (Huang & Hopper, 2016). Beyond that, tRNAs charged with cognate amino acids have been employed for labelling newly translated proteins for degradation, biosynthesis of antibiotics, modifications of cell membrane phospholipids, and creation of ribosomal peptide bonds (Raina et al., 2014).

In the context of tRNA biosynthesis, RNA polymerase III is responsible for transcribing eukaryotic tRNAs and ultimately creating precursor molecules (pre-tRNA). The pre-tRNAs are subsequently subjected to a series of post-transcriptional modifications to become mature tRNAs bearing a unique structural feature (Hopper & Huang, 2015).

In the two-dimensional model, from 5′ to 3′ direction, the tRNA is composed of several important parts: the acceptor stem, the D-arm, the anticodon stem, the variable loop, and the T-arm (Figure 1). Each individual component further features a specific function. The three-base anticodon, located at the acceptor stem, is responsible for the specificity of the complementary base pairing with the corresponding mRNA sequence. The stabilization of the tertiary structure is facilitated by the D-arm, which is named after the presence of a dihydrouridine base in the loop. Lastly, the T-arm, also referred to as the TΨC arm, comprises the universally conserved modified bases thymidine, pseudouridine, and cytidine, from which its name is derived, and is necessary for promoting interactions with the ribosome. The intramolecular interactions between the T-arm and the D-arm are required for the proper folding of tRNA into an L-shaped three-dimensional structure (Figure 1) (Berg & Brandl, 2021).

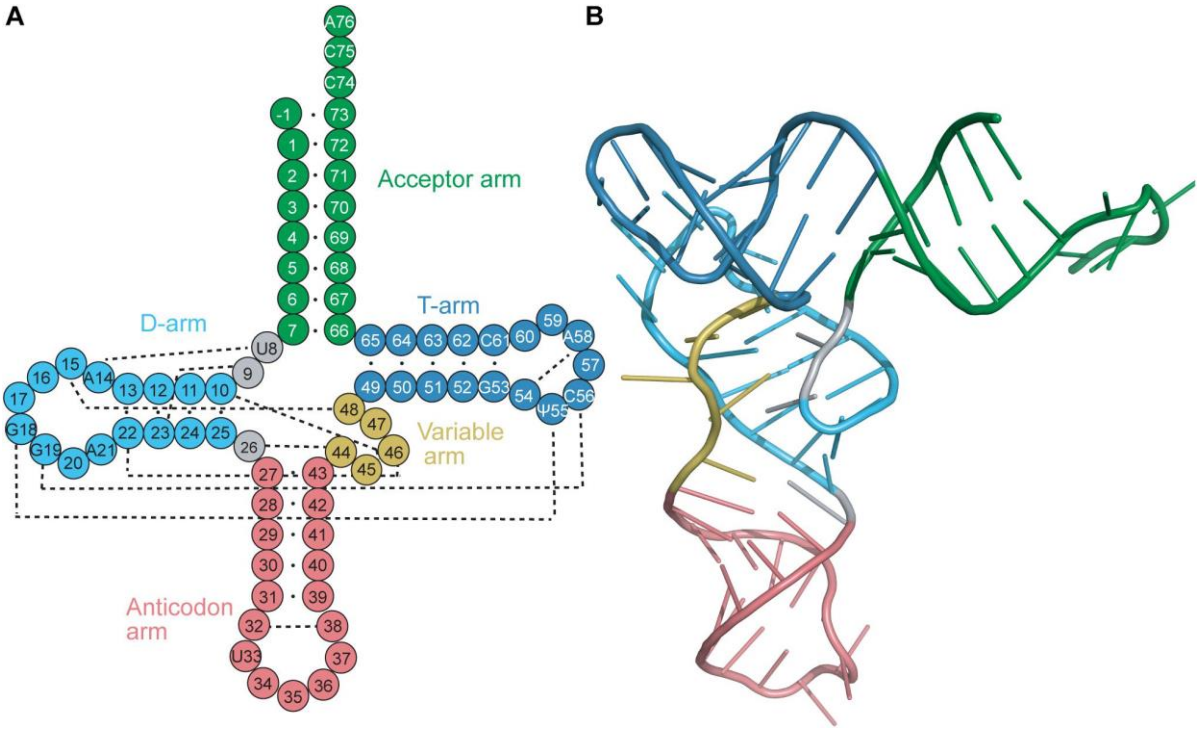

Figure 1. *(A) Secondary structure (cloverleaf) of mature tRNA with conventional tRNA numbering. (B) Three-dimensional L- shaped structure of mature tRNA. The different regions of both structures are colour coded: the acceptor stem is depicted in green, the D-arm in light blue, the anticodon arm in pink, the variable arm in yellow, and the T-arm in dark blue. The tertiary interactions forming the L-shape of tRNA are represented by a dashed line. From: (Krahn et al., 2020)*

To eventually become an adaptor molecule in translation, an aminoacyl-tRNA has to be formed by charging the tRNA isoacceptor with a cognate amino acid. These aminoacyl-charged tRNAs are fully functional for the incorporation of specific amino acids into the growing polypeptide chain, effectively becoming adaptor molecules in translation (Raina et al., 2014).

1.2. tRNA posttranscriptional modifications

Following transcription, the tRNAs are subjected to diverse post-transcriptional processing, including the removal of nucleotides on 5′ and 3′ ends, the addition of a nucleotide to all 3′ ends and to a specific 5′ end, intron removal in tRNA splicing, and modifications of nucleosides (Hopper, 2013).

The eukaryotic tRNAs generally possess 13 modifications per molecule, contrary to the bacterial tRNA, which typically comprises 8 modifications. Generally, modifications found

on the anticodon loop are necessary for influencing mRNA decoding, while modifications situated in other regions of tRNA influence stability, conformation, cellular placement, and quality control (Zhang et al., 2022).

One of these modifications is the hypermodified 7-deaza-guanosine, also known as queuosine (abbreviated to Q) (Figure 2) (Fergus et al., 2015). Q is located at the wobble position 34 of tRNAs bearing the 5′-GUN-3′ anticodon sequence. Hence, the queuosine modification is present in $tRNA^{His}$, $tRNA^{Asp}$, $tRNA^{Asn}$, and $tRNA^{Tyr}$ across eukaryotic and eubacterial organisms (Nishimura, 1983).

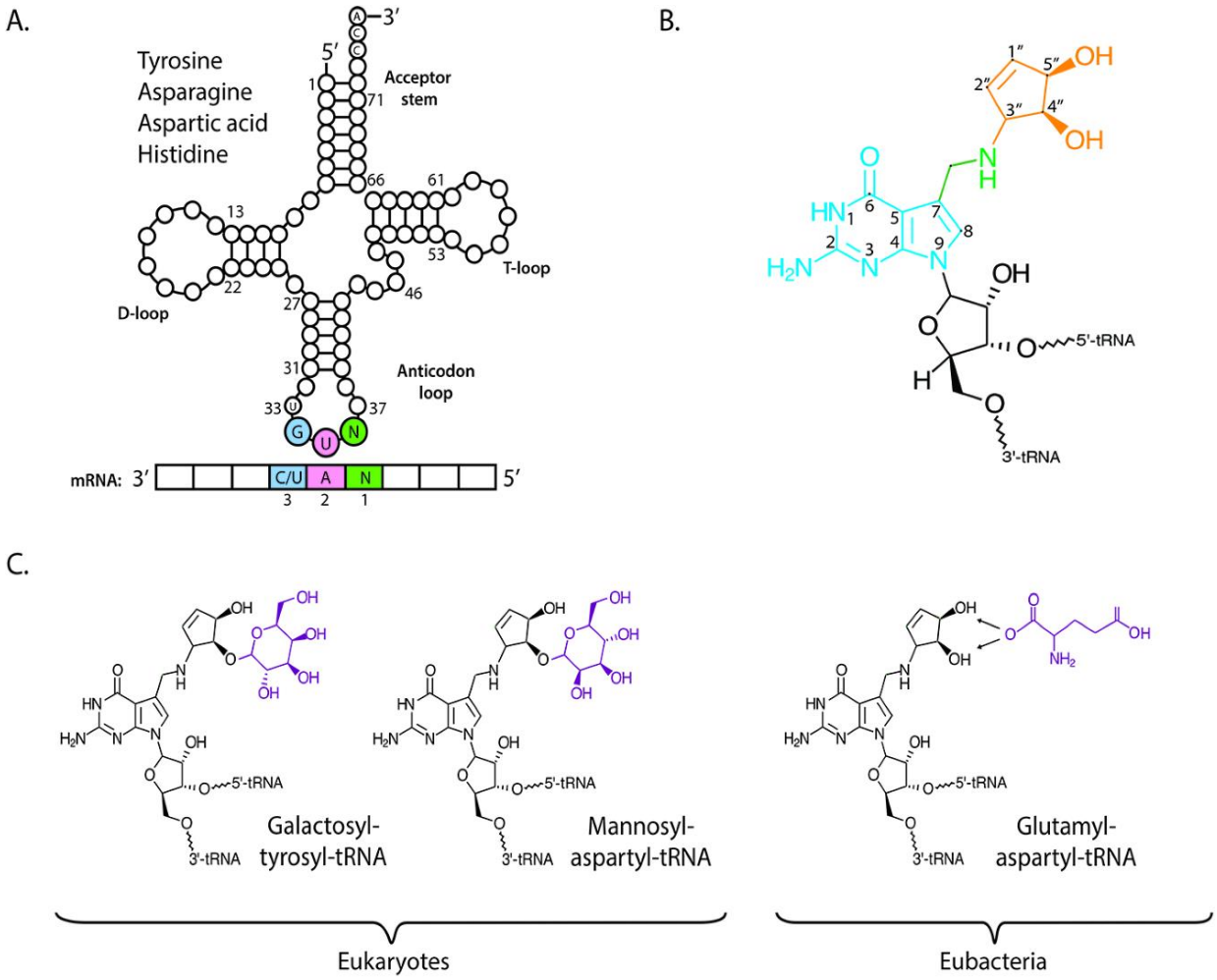

Figure 2. *(A) Anticodon structure of G34U35N36 tRNA, where N can be any base. (B) Queosine (7-(3,4-trans-4,5-cis-dihydroxy-1-cyclopenten-3-ylaminomethyl)-7-deazaguanosine) chemical structure. (C) Possible Queosine modifications. From: (Fergus et al., 2015).*

The modified base of the nucleoside queuosine is known as queuine (q) (Fergus et al., 2015). Bacteria can synthesize queuine *de novo* through a series of enzymatic reactions that involve the biosynthesis of pre-Q1. The G34 is then further substituted for pre-Q1 via a reaction catalysed by tRNA guanine transglycosylase (TGT). Conversely, the eukaryotes rely on dietary sources or gut microbes to obtain Q, and the guanosine is directly exchanged for queuine with the help of eukaryotic TGT (Phizicky & Hopper, 2023). The previous documentation of Q modifications in eukaryotes links its presence and absence to a variety of biological processes, including cancer, development, and tyrosine biosynthesis (Fergus et al., 2015).

1.3. tRNA trafficking

Trafficking of tRNA between the nucleus and cytoplasm belongs to processes crucial for proper cell functioning and viability. The transport of tRNAs does not begin until the newly transcribed pre-tRNAs are properly processed in the nucleus. After processing, tRNAs are exported to the cytoplasm, where the translation machinery is located. For a long time, this unidirectional nuclear export was thought to be the only pathway for tRNAs. However, it is now widely accepted that tRNAs are also transported back into the nucleus via a process called retrograde import to undergo further maturation steps. These mature tRNAs are then re-exported back to the cytoplasm (Figure 3) (Paris, 2021). Moreover, the distribution of tRNAs across different cellular compartments is found to be highly influenced by the cellular environment. For example, when the levels of amino acids (aa), glucose, or Pi are depleted, tRNA tends to accumulate in the nucleus (Hurto et al., 2007; Whitney et al., 2007).

The transport of the tRNAs, as for other macromolecules, occurs through the nuclear pore complex (NPC), which is embedded in the nuclear envelope. The NPC is composed of around 500-1000 hundred distinct proteins known as nucleoporins and serves as a pore through which transport is facilitated by interacting with the cargoes being transported (Dultz et al., 2022).

Transport through NPC can occur freely for molecules smaller than 40 kDa (Fried & Kutay, 2003), but must be facilitated with soluble nuclear transport factors (NTFs) for molecules larger than this diffusion limit. The NTFs mainly comprise factors of the karyopherin family. Based on their specific functions, the karyopherins are further subdivided into those responsible for export (exportins) from the nucleus to the cytoplasm, and those responsible for

import (importins). These proteins then shuttle via nuclear pores that penetrate the nuclear envelope (Pemberton & Paschal, 2005).

In addition to karyopherins, Ran GTP regulates nucleocytoplasmic transport. Ran exists in two forms, the GTP bound and the GDP bound, and controls the association and dissociation of the cargo complexes being transported (Fried & Kutay, 2003). When cargo is being exported from the nucleus to the cytoplasm, it binds to the exportin and Ran GTP located in the nucleus. Upon translocation through the NPCs, the Ran GAP promotes the hydrolysis of Ran GTP, which is linked to the release of the complex in the cytoplasm. On the contrary, when it comes to the import of cargo, the importin bound to cargo is transported into the nucleus, where the Ran GTP facilitates the dissociation of cargo in the nucleus (Pemberton & Paschal, 2005).

In the context of protein cofactors required for tRNA trafficking, in yeast, two major exportins, namely Los1 and Msn5, were found to be necessary to facilitate their export. Los1 was characterized to be mainly involved in primary export and re-export, as it interacts with both spliced and un-spliced tRNAs with no regard for these tRNAs being charged with amino acids. On the contrary, Msn5 is known to play a role in tRNA re-export, because it binds preferably to already spliced and amino acid-charged tRNAs. The homologs of Los1 and Msn5 in vertebrates are exportin-t (Xpo-t) and exportin-5 (Xpo-5) respectively (Paris, 2021). The function of Xpo-5, however, is shown to be minimal as it is primarily involved in the export of miRNAs (Calado et al., 2002).

The function of Los1 and Msn5 is undoubtedly important. However, the studies employing double mutants of these proteins showed that the functionality of the cells was not influenced, indicating that other pathways have to be involved in tRNA export (Huang & Hopper, 2015). Therefore, in addition to these two players in tRNA export, by utilizing a genome-wide screen, new potential candidates were identified. The heterodimeric complex of Mex67-Mtr2, already known for its role in the export of mRNAs, rose as a new candidate (Wu et al., 2015). The nuclear tRNA accumulation of end-maturated unspliced tRNAs occurs as a result of Mex67-Mtr2 inactivation. It is therefore believed that Mex67-Mtr2 and Los1 are important parts of primary tRNA export. Even though tRNA export was studied in many model systems, various important factors continue to be insufficiently explained (Chatterjee et al., 2017).

In *Trypanosoma brucei*, the knockdown of the canonical nuclear tRNA exporters TbXpo-t and TbXpo-5 did not initiate an accumulation of mature tRNAs in the nucleus, nor did it block the nuclear export of intron-containing tRNAs. Additionally, similarly to observations in yeast,

they were found to be unnecessary for cell viability. In order to identify different mechanisms for tRNA export in *T. brucei*, the knockdown of TbMex67-TbMtr2 was performed, which resulted in the accumulation of specific tRNA subsets in the nucleus. (Hegedűsová et al., 2019).

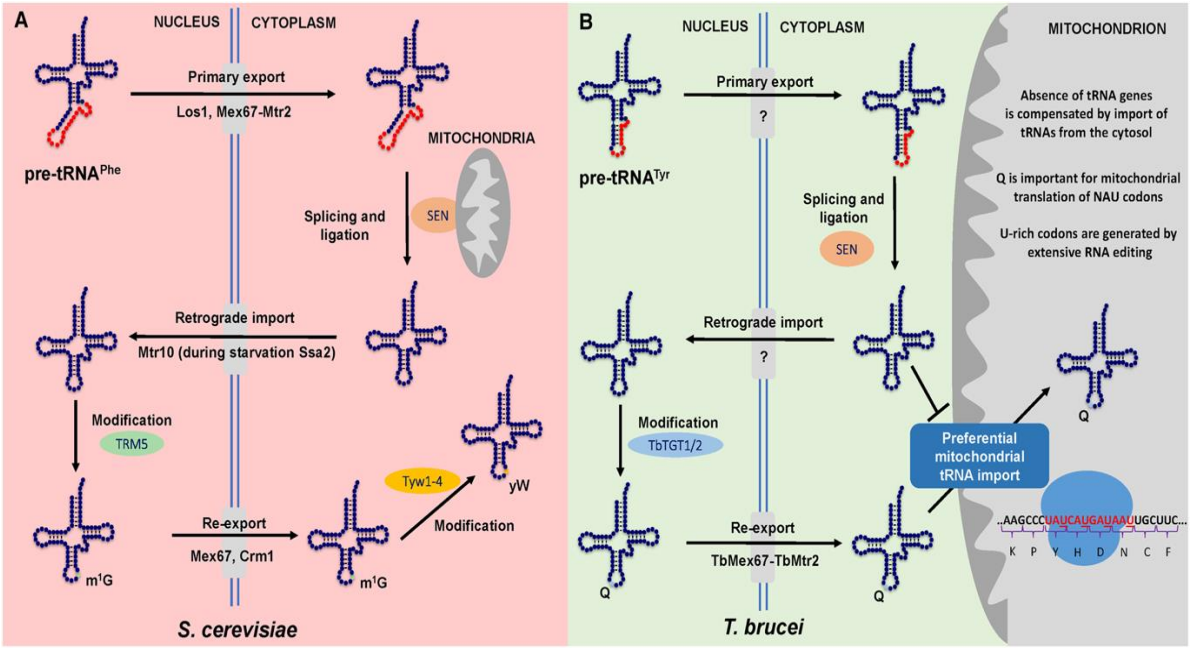

Figure 3. *tRNA trafficking. (A) Representation of tRNA^{Phe} retrograde nucleocytoplasmic transport in S. cerevisiae. (B) tRNA^{Tyr} trafficking in T. brucei. From: (Paris, 2021)*

1.4. tRNA retrograde pathway

The transformation of newly transcribed tRNA and mature tRNA includes several processes, including post-transcriptional modifications, trimming, and intron splicing. These processes take place within different compartments of the cell, making tRNA trafficking between the nucleus and cytoplasm crucial for tRNA processing (Kessler et al., 2018).

In the case of the import of cargo proteins, the importinα recognizes the nuclear localization signal (NLS) found on the protein being transported. The importinβ then binds to the importinα and facilitates the transport into the nucleus across the NPC. Moreover, it was found that importinβ is able to bind certain cargoes on its own and is capable of mediating the transport without the help of importinα (Harel & Forbes, 2004).

The tRNA retrograde pathway was first described in *Saccharomyces cerevisiae*, where it plays an important role in tRNA modification (Shaheen & Hopper, 2005), as the tRNAs comprising

an intron have to travel through the NPC to the outer mitochondrial surface, where the splicing endonuclease complex resides (Yoshihisa et al., 2003). Upon splicing of the tRNA intron, the tRNAs are transported back to the nucleus to undergo further modifications. After the necessary modifications in the nucleus, the tRNA is re-exported back to the cytoplasm to function as an adaptor molecule in translation (Ohira & Suzuki, 2011). Utilizing the HCl/aniline assay, Mtr10 was identified to play a role in $tRNA^{Phe}$ import. Additionally, it was shown that Mtr10 and Ssa2 play a role in $tRNA^{Phe}$ in conditions of amino acid deprivation (Nostramo & Hopper, 2020). Similarly, the import of specific tRNAs as a result of oxidative stress was also observed in human cells, where it was suggested to function as part of an integrated stress mechanism (Schwenzer et al., 2019).

Further supporting the significance of the tRNA retrograde pathway, the tRNA import was also suggested to be part of tRNA quality control (Kramer & Hopper, 2013). Moreover, the process of tRNA retro-translocation was proposed to have a protective effect against tRNA degradation when nutrient depletion occurs (Kessler et al., 2018).

Similarly to *S. cerevisiae,* in *T. brucei,* the splicing of intron-containing tRNA occurs in the cytoplasm. *T. brucei* possesses the only intron-containing tRNA ($tRNA^{Tyr}$). The mature form of the $tRNA^{Tyr}$ contains queosine modification at the third position of the anticodon. It has been demonstrated that only intronless $tRNA^{Tyr}$ can obtain Q modification, and therefore, first, the splicing in the cytoplasm has to take place. The spliced mature $tRNA^{Tyr}$ is subsequently transported back into the nucleus via the tRNA retrograde pathway in order to be modified with Q (Kessler et al., 2018). The Q-containing tRNA is re-exported by Mex67-Mtr2 from the nucleus to the cytoplasm to participate in proteosynthesis (Hegedűsová et al., 2019).

Even though the existence of the tRNA retrograde pathway is now fully accepted and has been observed in various organisms, including humans, its biological importance stays unclear (Paris, 2021). Moreover, the importins of the karyopherin family responsible for tRNA retrotranslocation remain unknown.

1.5. The model organism Trypanosoma brucei

Trypanosoma brucei, a causative agent of Human African Trypanosomiasis, is a protozoan parasite, which beyond its significance as a disease-causing agent, has emerged as a model organism employed for understanding fundamental questions in cell biology (Lukeš et al., 2023). The structure of the *T. brucei* genome is organized unusually, as various functionally non-related genes are grouped and result in a polycistronic transcript. Consequently, in comparison to other organisms, *T. brucei* has an absence of transcriptional regulation, and most of the gene expression is regulated post-transcriptionally. Moreover, these protists have a complex life cycle, including two hosts and major changes in metabolism and morphology (Fenn & Matthews, 2007). Owing to the complexity of its life cycle, in vitro studies of changes in signalling and cellular transformation across different life-cycle stages are possible (Li & He, 2017). By using a fully sequenced genome and diverse molecular techniques, it was possible to create loss of function and gain of function cell lines in *T. brucei*. In addition, a great number of molecular tools have been created to track alterations in these cell lines. As an outcome, new findings in molecular biology have been uncovered in cultured *T. brucei* (Ooi & Bastin, 2013). For instance, the discovery of the glycosylphosphatidylinositol (GPI) anchors (Ferguson et al., 1988) and the presence of base J (Gommers-Ampt, 1993). *T. brucei* also became a great model for protein functional analysis due to the use of inducible expression, or RNAi (Li & He, 2017).

In comparison to eukaryotes, kinetoplastid parasites bear unique features in gene expression. These comprise processes including mitochondrial RNA editing, import of mitochondrial tRNA, trans-splicing of polycistronic mRNAs, and dependence on posttranscriptional regulation because of the general absence of transcriptional promoters. The changes in nucleocytoplasmic tRNA pools as a reaction to conditions including nutrient depletion and oxidative stress imply that tRNA trafficking can be another posttranscriptional mechanism that influences gene regulation. Consequently, this might have a crucial impact on the life cycle of these parasites, as they face various changes in environments with different sources of nutrients with their transition between the mammalian and insect stages (Paris, 2021).

1.6. Hypothesis

The concept of tRNA trafficking is now widely accepted. While the function of the tRNA retrograde pathway has become clearer in the past years, the proteins facilitating the transport remain unknown. In this thesis, we therefore focus on uncovering the function of two potential candidates, Kap60 (accession number: Tb927.6.2640) and Kap95 (accession number: Tb927.10.2900) in tRNA retrograde transport. Kap60 and Kap95 are protein-coding genes found in *T. brucei*, containing an importin alpha subunit and an importin beta subunit, respectively. In addition, these proteins were identified by a collaborating laboratory (Dr. Samson Obado, Rockefeller University, USA) using mass spectrometry as NPC binding partners, which supported the selection of these candidates for our functional analysis. Generally, importins are responsible for recognising cargo being transported and facilitating the import in a Ran- dependent manner. The identification of the protein in the import family responsible for this transport may provide critical insight into tRNA trafficking and its influence on protein synthesis and cell viability.

2. Aims of the thesis

The overall aim of this thesis is to identify the components of the tRNA retrograde pathway in *T. brucei* by elucidating the function of protein-coding genes Kap60 and Kap95 using RNA interference.

The aims of the thesis include:

1. Generation of Kap60 and Kap95 knockdown constructs.
2. Electroporation of the constructs into the procyclic stage of *T. brucei.*
3. Confirmation of the RNAi cell lines in the *T. brucei.*
4. Testing for a role of Kap60 and Kap95 in the tRNA retrograde pathway.

3. Materials and Methods

3.1. Generating the RNAi knockdown constructs

To identify a possible role of the protein-coding genes Kap60 and Kap95 on the tRNA retrograde pathway, the silencing of their gene expression was performed using RNA interference (RNAi).

3.1.1. Primer design

To clone the genes of interest into an RNAi vector, the corresponding sequences were amplified from the *T. brucei* genomic DNA. For this purpose, the nucleotide sequences of the protein-coding genes KAP60 (accession number: Tb927.6.2640) and KAP95 (accession number: Tb927.10.2900) were obtained from the TriTryp database (tritrypdb.org). Using SnapGene software, four primers satisfying all our requirements, such as annealing temperature, length of the cloning fragment, and restriction site, were designed and ordered from Generi Biotech. The restriction site HindIII was chosen for forward primers and BamHI for the reverse ones (Table 1).

Table 1. Designed primers for Kap60 and Kap95.

Name	Sequence	Restriction site
ZP684F_KAP60-alpha Forward	5´CCCAAGCTTATGTTCAGTGGTCAGAATGA3´	HindIII
ZP685R_KAP60-alpha Reverse	5´CGGGATCCGACAGTCAGGACTAGGTGAA3´	BamHI
ZP686F_KAP95-beta Forward	5´CCCAAGCTTATGAGCTCCTTGACGGAATT3´	HindIII
ZP687R_KAP95-beta Reverse	5´CGGGATCCTGAGACTCCGTTGCACTTAT3´	BamHI

3.1.2. Polymerase chain reaction (PCR)

The Kap60 and Kap95 fragments were amplified from *T. brucei* genomic DNA using the designed primers (Table 1). The reaction mixtures were prepared according to Table 2 and placed into a PCR cycler (Table 4). During PCR, the Taq polymerase generated PCR products with A overhangs on the 3' end, which is required for the next step, the ligation into the pGEM- T-Easy vector.

Table 2. PCR reaction mixture.

Reagent	Stock concentration	Final concentration	Volume
Template DNA	1000ng/µl	4ng/µl	2 µl
Forward primer	10µM	0.4µM	2 µl
Reverse primer	10µM	0.4µM	2 µl
PCR master mix (Promega)	2X	1X	25 µl
ddH2O	-	-	19 µl

Table 3. PCR master mix (Promega).

Reagent	Concentration
Taq DNA polymerase (pH 8.5)	50units/ml
dNTPs	40µM
MgCl2	3mM

Table 4. PCR program.

Step	Temperature / °C	Time / s	Cycles
Initial denaturation	94	60	
Denaturation	94	0.15	Cycle :30
Annealing	63	0.15	
Elongation	72	0.45	
Final elongation	72	420	
Hold	12	infinite	

3.1.3. Agarose gel electrophoresis and PCR clean-up

Agarose gel electrophoresis was used to verify the length of the two PCR amplicons. The 1% agarose gel was prepared according to Table 5. Following the preparation, the gel was let to solidify before 7 µl of PCR product samples were loaded onto the wells. The gel electrophoresis was conducted at 100 V for 60 minutes. The ethidium bromide-stained bands were visualized with the Chemidoc Gel Imagining System from BioRad and ImageLab software. The size of the separated DNA was compared to a 1kb DNA ladder from Invitrogen.

Table 5. 1% Agarose gel mixture.

Reagents	Amount
Agarose	1 g
1XNNB	100 ml
Ethidium bromide (10 mg/mL)	1 µl

PCR products of the expected size were purified using the PCR purification kit provided by GeneAll. The concentration of the purified PCR product was determined using Nanodrop.

3.1.4. Ligation in pGEM-T-Easy vector

The products were further ligated into cloning-pGEM-T-Easy vectors (Promega) with complementary T-overhangs by mixing reactions as shown in Table 6. The pGEM T-Easy comprises a region that codes for B galactosidase, which further enables us to select the positive transformants of *E.coli*. The ligation mixtures were incubated for 60 minutes at room temperature.

Table 6. Ligation mixture.

Compound	Volume
T4 DNA ligase	1 µl
Vector (pGEM-T-Easy) 50 ng/µl	0.5 µl
2x Rapid Ligation Buffer	5 µl
PCR product (Kap60-42.2ng/µl, Kap95-43.1ng/µl)	0.33 µl Kap60 / 0.26 µl Kap95

3.1.5. Transformation

During transformation, the ligation mixture (5 µl) was mixed with the *E. coli* competent cells XL1-blue (50 µl). The mixture was then placed on ice for 20 minutes. Subsequently, the heat shock was performed by incubating the mixtures at 42°C for 45 seconds, followed by incubation on ice for 2 minutes. After the heat shock, SOC medium (900 µl) was added to the mixtures, and the samples were incubated for 60 minutes at 37 °C.

Following the incubation, the LB agar plates prepared with IPTG 15 (200 mg/ml), X-gal (20 mg/ml), and ampicillin (0.1 mg/ml) were used for the selection of positive transformants. After spreading the transformed cells onto the plates, the plates were incubated at 37 °C overnight. The next day, five individual colonies for each sample were chosen and replica plated before they were inoculated into 3 ml of LB broth containing ampicillin (0.1 mg/ml). The inoculated LB broths were incubated at 37 °C for 18 hours.

3.1.6. Isolation and purification of plasmid DNA

Plasmid DNA was isolated using the protocol GeneAll® Exprep™ Plasmid SV mini using manufacturer instructions. The concentration of plasmid DNA was determined using a NanoDrop spectrophotometer.

3.1.6.1 Control restriction digestion of plasmid DNA

The restriction reaction was performed to verify the presence of the target insert in the vector. The reactions were prepared according to Table 7 and incubated for two hours at 37°C.

Table 7. Restriction digestion mixtures.

Compound	Amount
10X Cut Smart Buffer	2 µl
HindIII	2 µl
BamHI	2 µl
plasmid DNA	1 µl
milliQ water	13 µl

The products of restriction digestion reactions were analysed using a 1% agarose gel. The separated inserts were visualized using the Chemidoc Gel Imagining System from BioRad and ImageLab software. The positive transformants were selected from each product, and each of them were grown in 2 tubes containing 5 ml of LB medium enriched with 0.1 mg/ml ampicillin.

3.1.7. Restriction digestion of plasmid DNA and p2t7-177 vector

Both PCR plasmids containing fragments of Kap60 and Kap95, as well as the p2t7-177 RNAi vector, were digested with BamHI and HindIII endonucleases. The mixtures were prepared according to Table 8. The digestion reaction was incubated at 37 °C overnight. To verify the product of the restriction reaction, 1% DNA agarose gel electrophoresis was performed.

Table 8. Restriction digestion mixture.

Compound	Kap60	Kap95	p2t7-177
10X Cut Smart Buffer	5 µl	5 µl	5 µl
HindIII	1 µl	1 µl	1 µl
BamHI	1 µl	1 µl	1 µl
DNA Kap60 (374ng/µl), Kap95 (203ng/µl), p2t7-177 (329 ng/µl)	10 µl	20 µl	12 µl
MilliQ water	33 µl	23 µl	31 µl

3.1.8. DNA extraction from gel

The entire volume of the restriction digestion reactions (50 µl) was mixed with 8 µl of 6x DNA loading dye and loaded on 1% agarose gel, which was prepared by dissolving 1g of agarose in 100 mL of 1x NNB electrophoresis buffer. As soon as the solution was cooled down, 1 µl of 10 mg/mL ethidium bromide (EtBr) was added.

The DNA fragments of the expected size were excised from the gel using a clean razor blade under a UV transluminator for visualization. Subsequently, DNA was purified using the Expin^{TM} Gel SV Protocol provided by GeneAll. The concentration of purified DNA was measured using a NanoDrop spectrophotometer.

3.1.9. Ligation of DNA fragments into p2t7-177 vector

For the generation of RNAi constructs, the p2t7-177 plasmid was used as a vector (Figure 4). This vector is commonly used for RNAi in *T. brucei* as it comprises a 177 bp sequence, which enables integration into transcriptionally silent minichromes of *T. brucei*. Additionally, it contains two TET-regulated T7 head-to-head promoters for the synthesis of dsRNA and phleomycin resistance for selection in *T. brucei*.

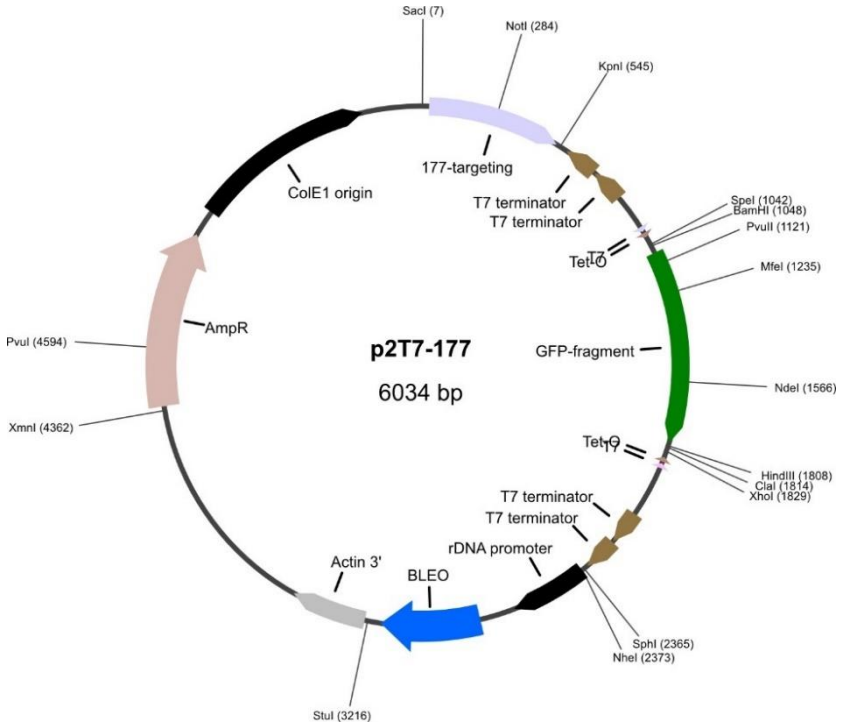

Figure 4. *Transfection RNAi vector p2t7-177 (Wickstead et al., 2002).*

The ligation reaction was used to ligate the Kap60 and Kap95 fragments into the p2t7-177 vector by the T4 DNA ligase enzyme. The molarity of each DNA molecule was calculated based on the obtained concentrations to establish the ligation reactions in a 3:1 molar ratio of insert to vector within a total volume of 10 µl. A negative control ligation with no insert DNA was carried out as well to assess the effectivity of ligation reactions. The ligation reactions (Table 9) were incubated overnight at 16°C. Following the incubation, inactivation at 65°C for 10 minutes was performed. Subsequently, the samples were placed on ice.

The ligated Kap60+p2t7-177 and Kap95+p2t7-177 constructs were transformed into the *E.coli* competent cells as previously described in 3.1.5. The positive clones containing recombinant plasmid were confirmed by restriction analysis using the same restriction enzymes, BamHI and HindIII, and the plasmid DNA was isolated as described in 3.1.6.

Table 9. Ligation mixture

Reagent	P2t7+KAP60	P2t7+KAP95	Blank
10x Ligation buffer	1 µl	1 µl	1 µl
T4 DNA Ligase	0.5 µl	0.5 µl	0.5 ul
insert	7.23 µl	2.65 µl	-
Vector	1.272 µl	1.272 µl	1.272 µl
ddH2O	-	4.58 µl	7.23 µl

3.2. Trypanosoma brucei transfection and selection

3.2.1. Linearization of plasmid with Not1

Linearization of the recombinant RNAi plasmid is required for correct insertion and integration into the parasite genome. Linearization reactions were prepared according to Table 10, and incubated overnight at 37°C.

To verify the linearization, 1% DNA agarose gel electrophoresis was performed, and the EtBr- stained bands were visualized using the Chemidoc Gel Imagining System from BioRad and ImageLab software. The resulting linearized constructs were precipitated by the addition of 3 volumes of 100% ethanol and 0.1 volume of 3M NaOAc.

Table 10. Linearization reaction mixture

Compound	KAP60	KAP95
Plasmid DNA	27 µl	26 µl
10x cut smart	20 µl	20 µl
Not1 enzyme	2 µl	2 µl
ddH20	151 µl	151 µl

3.2.2. Transfection into *Trypanosoma brucei*

5×10^7 procyclic *T. brucei* cells of the 29-13 strain were harvested at the mid-log phase by centrifugation at 3000 rpm for 10 minutes at 4°C. The resulting cell pellet was further resuspended in 100 µl of the master mix (Table 11), containing 10 µg of linearized DNA construct. The mixture was then transferred into a cuvette, and cells were electroporated with an AMAXA Nucleofector using the X-014 program for procyclic *T. brucei* forms. Following electroporation, cells were immediately transferred into a flask with 5 ml of SDM-79 media supplemented with 10% FBS and enriched with hygromycin (50 µg/ml) and geneticin (15 µg/ml). The cells were incubated for 16 hours at 27°C. Following the incubation, an additional 5 ml of medium was added, containing 5 µg/ml of the selectable antibiotic phleomycin.

For the selection of positive clones, the cells were distributed to 24 well plates. The wells in the first row of the plate were filled with 1.5 ml of the transfected cell culture. The second and third rows were filled with 1 ml of fresh SDM 79 (10% FBS, 50 µg/ml hygromycin, 15 µg/ml geneticin, 2.5 µg/ml phleomycin). The fourth row was filled with 0.5 ml of fresh SDM 79 (10% FBS, 50 µg/ml hygromycin, 15 µg/ml geneticin, 2.5 µg/ml phleomycin). 0.5 ml from

each well in the first row was pipetted into the corresponding wells in the second row and mixed by pipetting. Similarly, 0.5 ml from each well in the second row was transferred into the corresponding wells in the third row and mixed. Next, 0.5 ml from each well in the third row was transferred into the corresponding wells in the fourth row and mixed. The plate was kept at 27 ℃ until the mock transformants were eliminated by phleomycin selection.

The wells were inspected daily for positive clones using a bright field microscope. After 12-14 days, the clones were selected and transferred into a 25 cm^2 flask containing the SDM-79 medium (10% FBS, 50 µg/ml hygromycin, 15 µg/ml geneticin, 2.5 µg/ml phleomycin).

Table 11. Master mix electroporation mixture.

Compound	Amount
Human T-cell nucleofactor	82 µL
Supplement	18 µL

3.2.3. Growth curves

For every *T. brucei* clone, 10 ml cultures with a starting concentration of 1×10^6 cells/ml were prepared and kept at 27°C. The cells were induced by the addition of tetracycline and were counted every 24 hours by the Beckman Coulter Z2 Particle Counter. The concentration of the cells was kept at the mid-log phase by diluting the cells in a 1:10 ratio every time the concentration exceeded the concentration of 1×10^7 cells/ml. The measurement of cell densities was performed every 24 hours over a course of 5 days.

3.3. Verification of RNAi knockdown by RT-PCR

3.3.1. RNA isolation by guanidine extraction

The isolation of RNA from both Kap60 and Kap 95 *T.brucei* knockdown cell lines, 24 and 48 hours post induction was performed via guanidine extraction (Chomczynski & Sacchi, 2006).

Firstly, the cells were centrifuged at 3000 rpm for 10 minutes. The formed pellets were further resuspended in 1 ml of 1x PBS and transferred to the eppendorf tube. The contents of the tubes were spun again at 3000 rpm for 10 minutes. Subsequently, the obtained pellets were dissolved in 500 µl of Solution D (Table 12). The samples were then vortexed until the solutions were clear. Upon vertexing, 500 µl of NaOAC (pH 4.0), 500 µl of Phenol (H_2O saturated), and

150 µl of chloroform/IAA (24:1) were added. The samples were mixed by vortexing for one minute, followed by incubation on ice for 10 minutes. Afterward, the tubes were spun at 12000 rpm at 4°C. The supernatant was then transferred to a fresh tube, followed by the addition of an equal volume of isopropanol and 1 µl of glycogen (20 mg/ml). The samples were then stored at -20°C for 2 hours. After 2 hours, the stored samples were spun at 15000 rpm for 30 minutes at 8°C. The obtained pellet was washed with 150 µl of 70% ethanol and centrifuged at 15000 rpm for 5 minutes, followed by air-drying of the pellets for 3 minutes. The formed dried pellets were dissolved in 100 µl of MilliQ water. Subsequently, 0.5V of phenol (pH 8.0) and 0.5 V of chloroform /IAA (24:1) were added, and suspensions were vortexed for 1 minute. After mixing, a 10-minute incubation on ice was performed. Afterwards, samples were spun at 12000 rpm at 4°C for 30 minutes. The supernatant was transferred into new eppendorf tubes and precipitated with 3 V of ethanol, 0.1 V of 3 M NaOAc (pH 5.2), and 1 µl glycogen. The samples were then stored at -20°C overnight.

The next day, samples were spun for 30 minutes at 4°C. Formed pellets were washed with 150 µl of 70% ethanol and spun at 15000 rpm for 5 minutes. The obtained pellets were let to air-dry before being resuspendended in 30 µl of MilliQ water. To dissolve the RNA completely, samples were heated at 56°C for 10 minutes.

The RNA concentration was measured using a NanoDrop spectrophotometer.

Table 12. Solution D composition.

Substance	Concentration
Guanidine isothiocyanate	4 M
Sodium citrate (pH 7.0)	25 mM
Sarcosyl	0.5%
ß-mercaptoethanol	0.1 M

3.3.2. RT-PCR

To form template DNA for the PCR reaction, a cDNA had to be made. cDNA was prepared according to the QuantiTect Reverse Transcription Kit provided by Qiagen using manufacturer's instructions.

To verify the function of the knockdown construct in the cell line, PCR was performed on the formed template cDNA to confirm the decrease in mRNA transcript in the induced cells. For this purpose, the primers complementary to protein-coding genes Kap60 and Kap95 were

designed using SnapGene and ordered from Generi Biotech (Table 13). The PCR cycler was set according to Table 14. The products of PCR reactions were visualized using 1% DNA agarose gel electrophoresis.

Table 13. Primers for RT-PCR reaction.

Name	Sequence
ZP695F-alpha Forward	5´ TTTCATTCGCGCTAAACGGTA 3´
ZP696R-alpha Reverse	5´ TTACTCGTTTGCTCGACTATT 3´
ZP697F-beta Forward	5´ ATGAAGAGGCACATGGAGA 3´
ZP698R-beta Reverse	5´ CACTTCTCACCTAACCGTATTA 3´

Table 14. RT-PCR reaction cycle settings.

Step	Temperature / °C	Time / s	Cycles
Initial Denaturation	94	60	
Denaturation	94	0.15	35 X
Annealing	52	0.15	
Elongation	72	0.30	
Final Elongation	72	420	
Hold	12	∞	

To verify that samples were loaded equally, loading control with beta tubulin was performed. Table 15 and 16 display used primers and PCR setting respectively.

Table 15. Primers for tubulin.

Name	Sequence
ZP189F	5´ GCAGAGTCCAACATGAACGA 3´
ZP190R	5´ CGTCCGCGTCTAGTATTGCT 3´

Table 16. PCR reaction cycle settings for loading control with tubulin.

Step	Temperature / °C	Time / s	Cycles
Initial Denaturation	94	120	
Denaturation	94	0.15	25 X
Annealing	62	0.15	
Elongation	72	0.30	
Final Elongation	72	420	
Hold	12	∞	

3.4. Northern blot analysis

3.4.1. APB affinity gel electrophoresis

The levels of queosine-modified tRNAs and their alteration between RNAi-induced and uninduced cell lines were determined using affinity northern blot analysis. For this purpose, a gel was prepared by dissolving 25 mg of aminophenylboronic acid in 10 ml of 1x TAE gel solution (8 M Urea, 8% AA). The polymerization of the gel was triggered by the addition of 60 µl of 10% APS and 10 µL of TEMED. The prepared solution was then quickly shaken and transferred into a Biorad mini-gel apparatus.

To prepare the samples, 5 µg of total RNA was deacetylated by the addition of 5 µl of 1 M TRIS-HCl (pH 9.0). Subsequently, water was added to achieve a final volume of 50 µl and samples were incubated for 30 minutes at 37 °C. Following the incubation, samples were precipitated with 150 µl of 100% EtOH, 5 µl of 3M NaOAc, and 1 µl glycogen and stored at -20°C for 30 minutes. Afterwards, the samples were spun for 30 minutes at 15 000 rpm and washed with 70% ethanol.

Additionally, the periodate oxidation control had to be prepared. This was done by deacetylating the additional sample analogously to the rest of the samples and resuspending the formed pellet in 50 mM NaOAc (pH 5) and 2.5 mM $NaIO_4$. The prepared sample was then incubated for 2 hours at 37 °C in the dark. After 2 hours, 1 µl of 100 mM glucose was added to stop the reaction, and the sample was incubated for an additional 30 minutes at 37 °C. Following the incubation, the sample was purified via a Sephadex G-25 column. The purified sample was precipitated with ethanol before being spun for 30 minutes at 15 000 rpm. Lastly, a washing step with 70% ethanol was performed.

All prepared samples were resuspended in 6 µl of urea loading buffer and subsequently denaturated for 10 minutes at 70 °C. The prepared samples were then loaded onto the gel. The gel was run in 1x TAE buffer at 75 V at 4 °C for 6 hours. The RNA was visualized by staining the gel with ethidium bromide. The gel was visualized using the Chemidoc Gel Imagining System from BioRad and ImageLab software. Then the gel was destained for 15 min in 1X TAE on a shaking platform.

The RNA was blotted on ZETA probe membrane from BioRad by wet transfer in 0.5x TAE at 150 mA for 90 min. The membrane was dried and UV-crosslinked two times for 1 minute.

3.4.2. Oligonucleotide hybridization

To visualize $tRNA^{Tyr}$, oligonucleotide probes (Table 18) were labelled with a radioactive [gamma32P]-ATP isotope. To insert the P32 into the 5'-end of the DNA oligo, the oligo labelling reaction mixture was prepared according to Table 17 and incubated for 1.5 hours at 37 °C. Following the incubation, 90 µl of water was added, and the sample was further purified via a Sephadex G25 column. The oligo probe was then denaturated by heating at 95°C for 5 min.

The membrane was prehybridized for 45 minutes in 5 ml of hybridization solution (Table 20). After hybridization, the denaturated oligo probe was transferred into the hybridization solution, and the membrane was hybridized overnight at 48°C.

The next day, the probe was collected in a 15 ml tube, and the membrane was washed. For washing the membrane, first Wash 1 (Table 22) was applied, and the tube was inverted a few times before the solution was discarded. The next washing step was performed by applying 10 ml of Wash 1+Denh.sol (Table 23) for 20 minutes at 48°C. Afterward, the washing was repeated with Wash 2 (Table 24). The membrane was subsequently placed on wet filter paper, covered with plastic foil, and exposed to the Phosphoimager cassette overnight.

To develop the cassette, the Typhoon^{TM} 9410 scanner was used. Subsequently, the membrane was stripped by boiling at 80 °C twice for 30 min in a stripping solution (Table 25). The stripped membrane was then stored in a stripping solution at RT.

To verify that samples were loaded equally, hybridization of the same membrane with $tRNA^{Glu}$ (Table 19) was performed.

Table 17. Oligonucleotide labelling reaction.

Compound	Volume / µl
Oligonucleotide	1 (25 ng)
10x PNK buffer	1
10x T4 Polynucleotide kinase	1
gamma32P-ATP	1
MilliQ water	6

Table 18. Oligonucleotide used for norther blot analysis.

Name	tRNA	Anticodon	Sequence
ZP377R	tyrosine	GUA	5´ GTGGTCCTTCCGGCCGGAATCGAA 3´

Table 19. Oligonucleotide used for loading control.

Name	tRNA	Anticodon	Sequence
ZP07R	Glutamic acid	UUC	5´ TTCCGGTACCGGGAATCGAAC 3´

Table 20. Hybridization solution composition.

Hybridization solution	
Compound	**Amount**
20x SSC	125ml
1M Pi Ph7.2	10ml
SDS	35 g
100x Denhards solution	5 ml
Salmon sperm DNA	500 mg
Water	Up to 500 ml

Table 21. Composition of 100x Denhardt's solution.

100x Denhardt's solution	
Compound	**Concentration**
Ficoll 400	2%
Polyvinylpyrrolidone	2%
Bovine Serum Albumine	2%

Table 22. Composition of Wash 1 solution.

Wash 1	
Compound	**Amount**
20x SSC	150 ml
10% SDS	500 ml
1 M NaH_2PO_4 pH=7.5	25 ml
Water	325 ml

Table 23. Composition of Wash 1 with Denhardt's solution.

Wash 1 + Denh.sol.	
Compound	**Amount**
100x Denhardt's solution	20 ml
Wash 1	180 ml

Table 24. Composition of Wash 2.

Wash 2	
Compound	**Amount**
20x SSC	50 ml
20% SDS	50 ml
Water	900 ml

Table 25. Composition of stripping solution.

Stripping solution	
Compound	**Volume**
20x SSC	50 ml
10% SDS	10 ml
Water	985 ml

3.5. Fluorescence *in situ* hybridization

The *T. brucei* 1×10^7 cells from all studied cell lines were collected and harvested for 5 minutes at 3000 rpm by centrifugation. The obtained pellet was washed with PBS and further dissolved in 600 µl of a 4% paraformaldehyde/PBS solution. Subsequently, the fixation of the mixture on poly-L-lysine coated microscope slides was performed. This was done by applying 400 µl of resuspended cells to the slide. The slides were then left to dry for 30 minutes. Afterward, the non-attached cells were washed away with PBS, followed by dehydration of the attached cells. The dehydration was performed by sequentially applying 5%, 80% and 100% EtOH for a period of 3 minutes.

The permeabilized cells were then further pre-hybridized for two hours with a hybridization solution (Table 26). Following pre-hybridization, incubation at room temperature was performed overnight in a humid chamber by applying a hybridization solution containing 10 ng/µl of the Cy3 -$tRNA^{Tyr}$ (Table 27) probe and covering the slide with parafilm.

The next day, washing of the slides for 10 min was performed, by placing slide once with 4 × SSC with 35% deionized formamide, once with 2× SSC, and once with 1× SSC, onto a shaker for 10 minutes each. Lastly, the mounting medium containing 4′,6-diamino-2-phenylindole dihydrochloride (DAPI) was mounted onto the slides and covered with a coverslip. The cells were visualized using the Olympus FluoView™ FV1000 confocal microscope. The analysis of the obtained images was performed using Fluoview and ImageJ (NIH) software.

Table 26. Composition of FISH hybridization solution.

Initial Concentration	Final concentration
10 % BSA	2% BSA
100x Denhardt	5x Denhardt´s solution
20x SSC	4x SSC
20% dextran sulphate	5% dextran sulphate
100% deionized formamide	35% deionized formamide
40U/µl RNase inhibitor	10U/ml RNase inhibitor

Table 27. Used oligo for FISH.

Name	Sequence
ZP159R-Tyr(GUA)-mat-5end-Cy3	5'AACCAGCGACCCTGTGATCTAC 3'

3.6. Queosine starvation experiment

The *T. brucei* cells were cultivated in SDM-79 medium supplemented with 10% FBS. 1×10^8 cells were then centrifuged at 3000 rpm for 4 minutes. The resulting pellets were washed with fresh medium with no FBS and centrifuged again. The supernatant was discarded, and the cells were transferred into 20ml of SDM-79 supplemented with dialyzed FBS for an additional two days, with cell counting performed every 24 hours. After 48 hours in dialyzed medium, RNA was isolated, and the RNAi was induced by tetracycline.

After 24 hours of induction, the queuine was added to all flasks to a final concentration of 20 nM. After 24 hours upon the addition of queuiene, the RNA was isolated from all tested cell lines.

Moreover, the experiment was repeated with additional time points, where q was added 48 hours after induction and RNA was isolated 3 and 6 hours after the addition of q. The RNA was isolated by guanidine extraction, as previously described in 3.3.1. Lastly, the northern blot analysis was performed following the procedure outlined in 3.4.

4. Results

4.1. Generating the RNAi knockdown constructs

To generate the RNAi cell lines for each protein-coding gene (Kap60 and Kap95) in the procyclic stage of *T. brucei*, the parts of the target genes were amplified using PCR from genomic DNA using corresponding primers. The PCR products Kap60 and Kap95, with sizes of 551 bp and 431 bp, respectively, were ligated into the pGEM-T-Easy vector. The ligated products were transformed into *E. coli* competent cells, and positive clones were selected using blue-white screening. The positive transformants were confirmed by restriction analysis of the plasmid DNA. The Kap60 and Kap90 in the PCR vector as well as the p2t7-177 RNAi vector were both digested with the same restriction enzymes and ligated in the p2t7-177 vector. The ligation product was transformed into *E. coli,* and the positive transfectants were selected and confirmed by restriction analysis. The final RNAi constructs p2T7-177+Kap60 and p2T7- 177+Kap95 were linearized with Not1, prior to electroporation into the. *T. brucei* procyclic 29-13 WT strain.

4.2. Growth curves

To determine the influence of protein-coding genes Kap60 and Kap95 on the cell viability of PF *T. brucei* cell lines, growth curves were used. Consequently, we compared the growth rate of WT cells, uninduced cells, and RNAi-induced cells for both, Kap60 (Figure 5) and Kap95 (Figure 6). Cell density was evaluated daily, and cells were split to maintain the culture at mid- log growth. The growth rate of uninduced cells was plotted against that of RNAi-induced cells with the addition of tetracycline and WT cells. The resulting graphs show that after 48 hours of induction, the growth curves of both Kap60 and Kap95 induced cell lines began to show a strong growth phenotype.

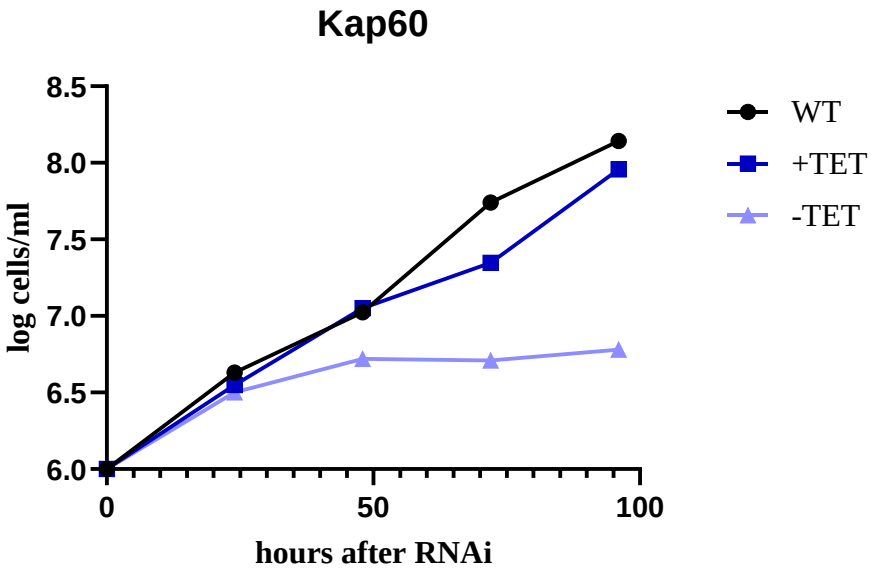

Figure 5. *Growth curve of induced and uninduced Kap 60 RNAi knockdown cell lines.*

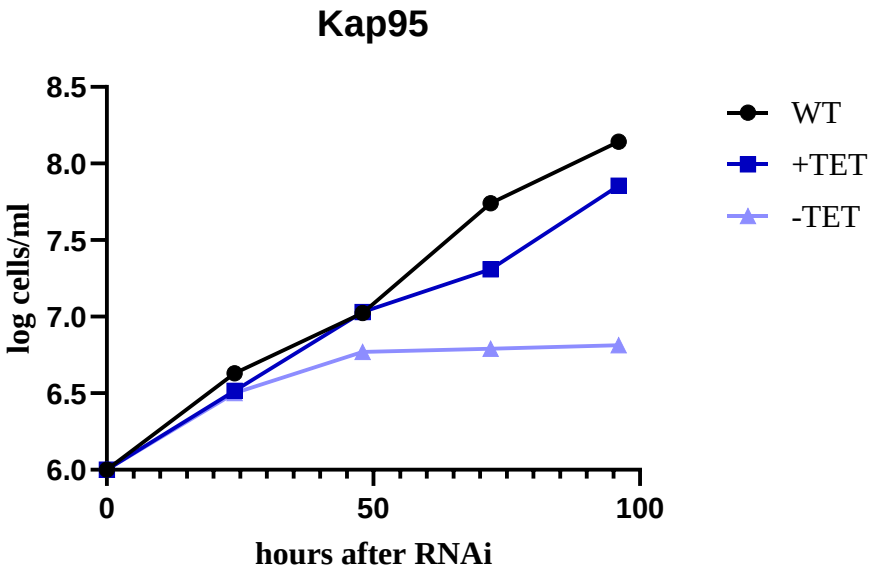

Figure 6. *Growth curve of induced and uninduced Kap 95 RNAi knockdown cell lines.*

4.3. Confirmation of Kap60 and Kap95 RNAi knockdown cell lines

For confirmation of Kap60 and Kap95 RNAi knockdown cell lines, RT-PCR was used. For these purposes, RNA was isolated from induced and uninduced cells 24 and 48 hours after induction. As a control, RNA was isolated from WT cells as well. The generated cDNAs served as a template for the PCR.

Significantly decreased levels in the mRNA transcript of the target gene were observed in PCR products of both RNAi induced Kap60 and Kap95 knockdown cell lines. The decrease in levels of mRNA transcript were more pronounced 48 hours after induction (Figure 7).

As a loading control, the primers for *T. brucei* tubulin beta were used, and PCR was performed using the same cDNAs as a template. Consequently, the PCR product was resolved on a 1% DNA agarose gel and visualized using Chemidoc Gel Imagining System from BioRad and ImageLab software (Figure 8).

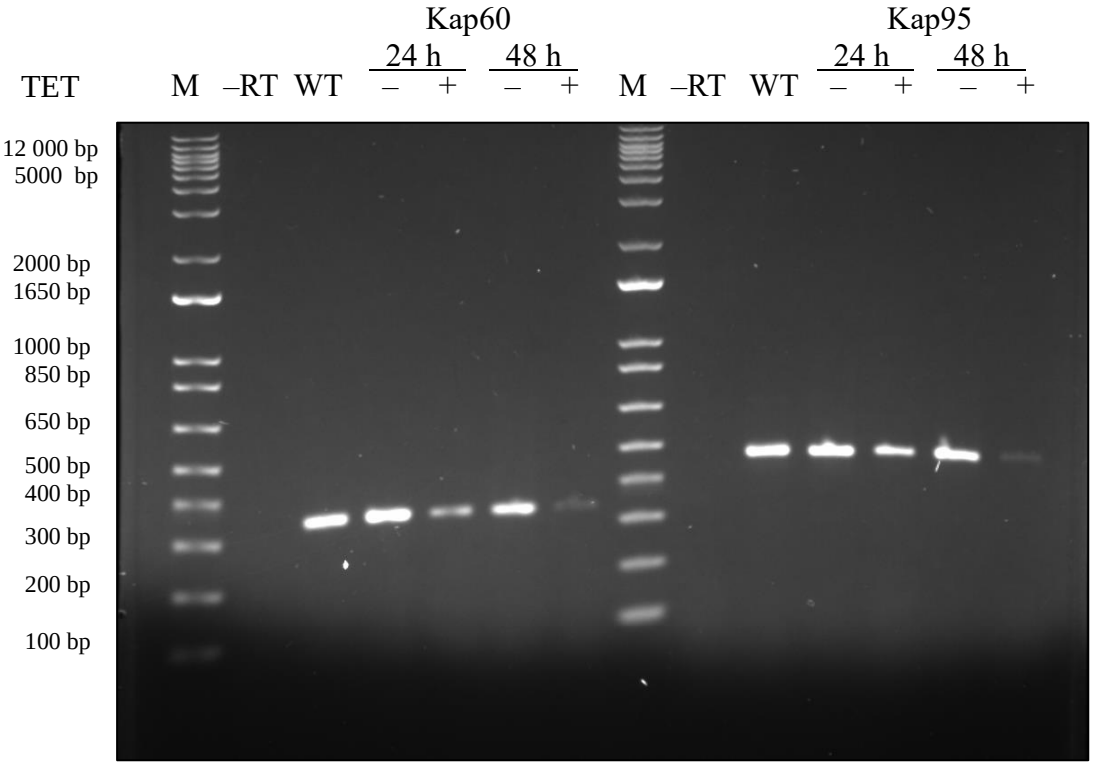

Figure 7. *RT- PCR of mRNA levels of Kap60 and Kap95 after RNAi.*

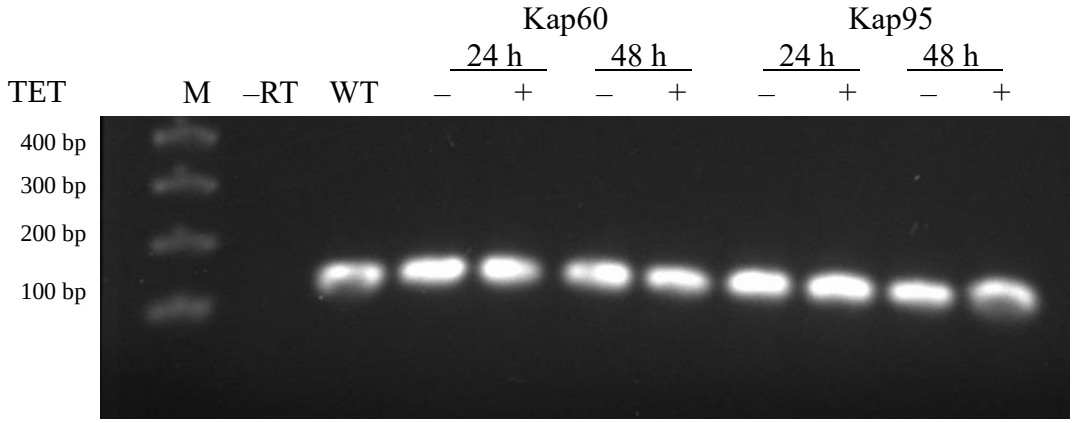

Figure 8. *RT-PCR of mRNA levels of tubulin was used as loading control.*

4.4. Determination of Q modified tRNA^{Tyr} levels in Kap60 and Kap95 RNAi cell lines

To identify whether Kap60 or Kap95 plays a role in the tRNA retrograde pathway, the levels of Q-modified tRNA^{Tyr} in RNAi induced and uninduced cell lines were determined. We took advantage, that the process of addition of Q modification takes place in the nucleus. In addition, the tRNA guanine transglycosylase, an enzyme responsible for this reaction, can act only on mature (spliced) tRNA. During its maturation process, the only intron-containing tRNA^{Tyr} has to be exported from the nucleus and spliced in the cytoplasm prior to being reimported and modified with Q. Hence, it was hypothesized that in the case of the potential effect of Kap60 or Kap95 on retrograde import of tRNA^{Tyr}, the northern blots should reveal lower levels of Q-modified tRNA^{Tyr} in both knockdown cell lines.

To detect Q-tRNA levels, aminophenyl boronate (APB) affinity PAGE followed by Northern blotting was performed. During APB affinity PAGE, the APB copolymerizes with the acrylamide and can bind with the cis-diol groups found in RNAs. These free cis-diol groups are present in the cyclopentene ring of Q-modified tRNAs and result in slower migration through the affinity gel. As a result, the separation of the tRNAs occurs in two bands, the unmodified (lower band) and the slower one being modified with Q (upper band). For negative control, periodate treated tRNA is utilized, as it oxidises the cis-diols. Consequently, the tRNAs treated with periodate travel the longest distance on the gel (Igloi & Kössel, 1985).

The RNA was isolated by guanidine extraction from wild type, induced, and uninduced cells, and cells 24 and 48 hours post induction.

The RNA was then blotted from the gel onto the ZETA membrane. Following blotting, hybridization with a $tRNA^{Tyr}$ complementary gamma 32P radiolabeled oligonucleotide probe was performed. The membrane was then subjected to exposure to a phosphoimager screen, and the Typhoon™ 9410 scanner was used to develop a phosphor storage signal.

In the case of the northern blot of the Kap60 cell line (Figure 9), the expected decrease in levels of Q-modified $tRNA^{Tyr}$ was not observed. Moreover, levels of Q-modified $tRNA^{Tyr}$ were slightly increased at both time points; 24 and 48 hours after induction. Similarly, in Kap95 cell lines (Figure 10), the levels of Q-modified $tRNA^{Tyr}$ did not alter between the induced and uninduced cell lines.

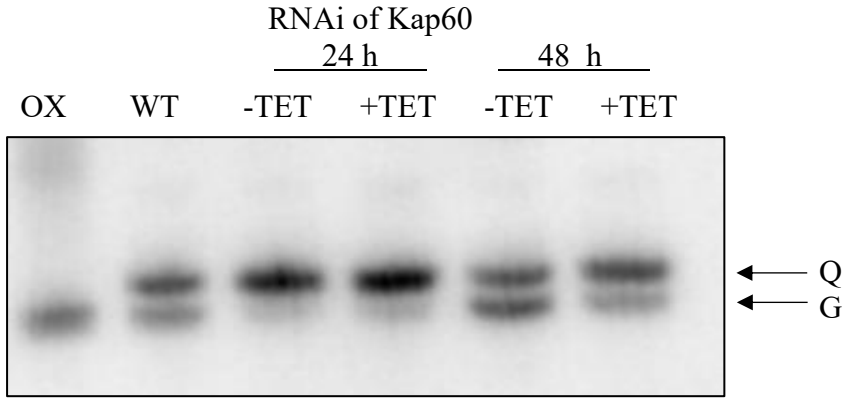

Figure 9. *APB Northern blot of Kap60 RNAi T. brucei cell lines.*

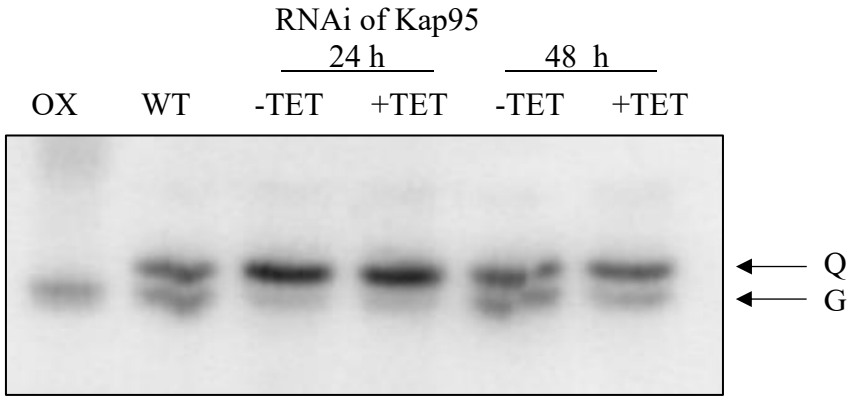

Figure 10. *APB Northern blot of Kap 95 RNAi T. brucei cell lines.*

4.5. Q starvation experiment

Given that the growth curve phenotype found in both knockdown cell lines is too pronounced, it was hypothesized that the effects of Kap60 and Kap95 on the tRNA retrograde pathway might be complicated to observe. This was based on the fact that the levels of Q-modified tRNAs could not be influenced by knockdowns in such a short time. Therefore, the Q- starvation experiment was carried out to test the hypothesis that Kap-60 and Kap-95 are responsible for tRNA retrograde import. In this experiment, Q levels were depleted before the induction process.

For these purposes, the cells were grown in a medium with dialyzed FBS, where low molecular weight molecules, including q, a precursor of Q, are absent. The cells were cultivated in dialyzed medium for two days prior to the induction. 24 hours after RNAi induction, the q was added. To follow, q-tRNA levels, the total RNA was isolated before induction, at the time of induction, and 24 hours after the addition of queine. In addition, the experiment was repeated with different time points, adding q 48 hours after induction and isolating RNA 3 and 6 hours after q addition.

After starvation of cells for q, there was successful depletion of Q-tRNA^{Tyr} in all cell lines. However, the expected alterations in Q-tRNA^{Tyr} levels between induced and uninduced knockdown cell lines after the addition of q were not observed in any of the experimental setups performed (Figure 11). Hence, these results indicate that neither Kap60 nor Kap95 block the re-import of Q-tRNA^{Tyr}, and thus the tRNA retrograde pathway seems to be equally functional in all tested cell lines.

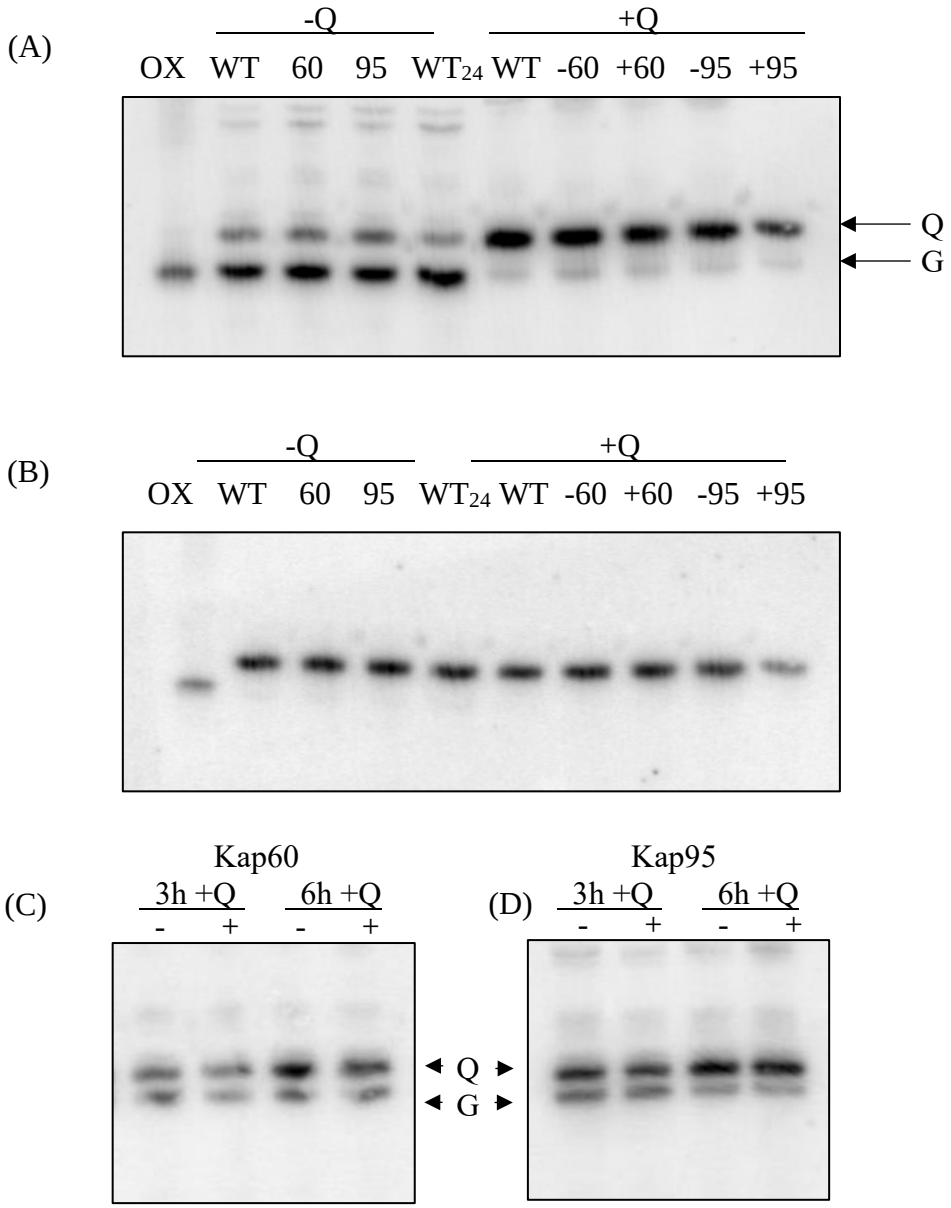

Figure 11. *(A) Northern blot after starvation. OX presents the negative control of oxidation by periodate. WT represents the positive control of the parental strain. WT_{24} represents a positive control after 24 hours of incubation in medium with dialyzed FBS. 60 represents the Kap60 RNAi cell line. 95 represents the Kap96 RNAi cell line. – and + represent RNAi induced and uninduced cell lines, respectively. -q represents medium with dialyzed FBS. +q represents medium supplemented with q. (B) Loading control of the same membrane. (C) Northern Blot of q starvation experiment in Kap60 RNAi cell lines, with RNA isolation 3 and 6 hours after the addition of q.*

4.6. FISH

Using fluorescence *in situ* hybridization, we aimed to observe the subcellular localisation of $tRNA^{Tyr}$ in the generated RNAi cell lines as well as wild types. Given the hypothesis that Kap60 and Kap95 are responsible for the tRNA retrograde pathway, a nucleus without fluorescently labelled $tRNA^{Tyr}$ was sought for observation. Moreover, using FISH, the influence of Kap60 and Kap95 on tRNA re-export could be examined. However, subcellular localisation of $tRNA^{Tyr}$ (Figure 12) showed no significant changes in the distribution of $tRNA^{Tyr}$ in cells after RNAi induction, suggesting that neither Kap 60 nor Kap 95 play a role in the nuclear import or re-export of $tRNA^{Tyr}$.

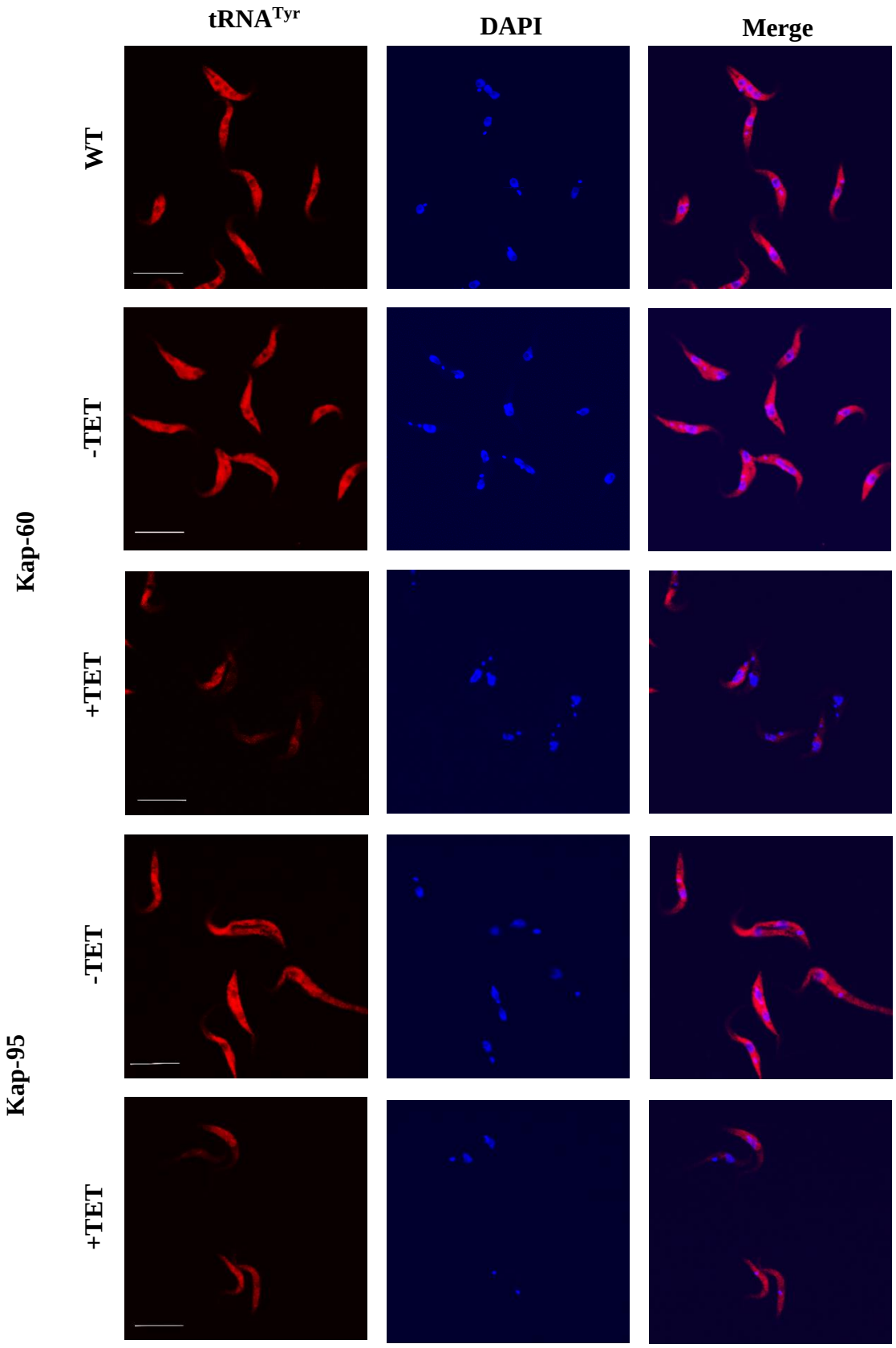

Figure 12. *Fluorescent in situ hybridization of Kap-60 and Kap-95 RNAi uninduced and induced T. brucei cell lines. In red. Cy-3, is the visualized subcellular localization of mature tRNA^{tyr}. DAPI was used for staining of kinetoplast and nucleus. Bars, 10 µm.*

5. Discussion

The objective of this thesis was to elucidate the role of protein-coding genes Kap60 and Kap95 on the tRNA retrograde pathway in *T. brucei*. Using an RNAi approach, we aimed to elucidate whether these two candidates are the key components for the re-import of $tRNA^{Tyr}$ into the nucleus.

The tRNA retrograde pathway is now well-accepted but remains a poorly characterized process conserved across a range of organisms. Since the discovery of the tRNA retrograde pathway in budding yeast, various functions have been connected to this process. These include tRNA quality control or maturation (Chatterjee et al., 2018). In *S.cerevisiae*, the tRNA retrograde pathway is necessary for the maturation of $tRNA^{Phe}$, as this process is mediated by the enzyme Trm5 found in the nucleus, which only methylates G37 on intron-less tRNAs. Since $tRNA^{Phe}$ comprises an intron, its export to the cytoplasm to get spliced, followed by import into the nucleus, is necessary (Ohira & Suzuki, 2011). Additionally, many cellular functions are affected by the tRNA import, such as cell cycle control and translation control (Chatterjee et al., 2018). Hence, an understanding of this process and its components is necessary for broadening our understanding of the impact of tRNA import on the biology of the cell.

In this thesis, we employed RNA interference (RNAi) as a strategy for the silencing of target genes, a technique that is routinely used for the identification of protein function. By applying this approach, we generated two Tet-inducible RNAi knockdown cell lines targeting either Kap60 or Kap95. We were able to verify the silencing of the corresponding transcripts on the mRNA level, and we observed a strong growth phenotype in both cell lines, where the inhibition in the growth of cell culture started to be evident within 48 hours post-induction. The poor viability and growth defects of these cell lines thus indicate that both of the genes are essential for the proper functioning of *T. brucei*. Furthermore, it was hypothesised that the target genes are responsible for facilitating tRNA retrograde import.

To perform a functional analysis of the candidate genes for their possible role in the tRNA retrograde pathway, we took advantage of two processing steps of the $tRNA^{Tyr}$, namely the cytosolic splicing of the tRNA intron and nuclear Q tRNA modification, which served as subcellular markers to follow the fate of this tRNA.

Therefore, it was hypothesized that the Kap60 or Kap95 would block the import of the spliced $tRNA^{Tyr}$ from the cytosol to the nucleus, preventing the $tRNA^{Tyr}$ from obtaining the Q. However, the expected alterations in levels of Q-$tRNA^{Tyr}$ were not observed after RNAi silencing, indicating that the tRNA retrograde pathway was still fully functional. We further speculated, that given the strong growth inhibition observed in both RNAi cell lines within both 24 and 48 hours, the inhibition of retrograde import may not be observable in such a short time frame. However, we were unable to isolate RNA from viable, healthy cells after more than 48 hours due to the strong growth phenotype. Therefore, the Q starvation experiment was designed to deplete Q from the media by using dialyzed FBS, resulting in significantly lower Q-tRNA levels prior to RNAi induction. After RNAi induction, queuine was added directly to the culture media. With this strategy, we hoped to achieve a more sensitive, detectable difference in Q-$tRNA^{Tyr}$ levels. However, this was not confirmed, and we did not see any differences in Q-levels of Q-tRNA between WT, RNAi uninduced, and induced cell lines.

Finally, we wanted to visualize the distribution of mature $tRNA^{Tyr}$ in the generated RNAi knockdown cell lines between the nucleus and cytosol. For this purpose, we used FISH (fluorescence in situ hybridization). It was expected that if the candidate genes are involved in tRNA retrograde import, we would not see an absence of the signal corresponding to the mature (spliced) form of $tRNA^{Tyr}$ in the nucleus compared to uninduced cell lines or WT, where the signal is expected throughout the cell. However, in agreement with the previous results, we did not observe any changes in the subcellular localization of $tRNA^{Tyr}$ after silencing Kap60 and Kap95. Additionally, by visualizing the subcellular localization of $tRNA^{Tyr}$, we were able to assess the influence of the two candidates, Kap60 and Kap95, on $tRNA^{Tyr}$ re-export, another pathway of tRNA trafficking. As previously documented by Hegedűsová et al. (2019), downregulation of the mRNA exporter TbMex67 led to nuclear accumulation of spliced $tRNA^{Tyr}$ in *T. brucei*, which was clearly observed by FISH. However, this observation was not replicated in the Kap60 and Kap95 RNAi cell lines tested, suggesting that neither Kap60 nor Kap95 are involved in the re-export of $tRNA^{Tyr}$.

Hence, our results indicate that Kap60 and Kap95 are not key components of the tRNA retrograde pathway. However, owing to their strong growth phenotype, these two karyopherins might be responsible for the transport pathways of other RNA molecules, such as rRNA or mRNA. Consequently, the key components of the tRNA retrograde pathway in *T. brucei* remain unknown.

6. Conclusions

In conclusion, the objective of this thesis was to elucidate the role of protein-coding genes Kap60 and Kap95 on the tRNA retrograde pathway. To this end, RNAi knockdown cell lines were generated. The results demonstrated a strong effect of the knockdown on the cell viability of both RNAi cell lines. By combining northern blot and FISH methods, we have demonstrated that these proteins do not participate in the tRNA retrograde import pathway. The findings indicate that Kap60 and Kap95 may possess additional functions within a transport pathway that remains to be fully elucidated.

Bibliography

Berg, M. D., & Brandl, C. J. (2021). Transfer RNAs: diversity in form and function. *RNA Biology*, *18*(3), 316–339. https://doi.org/10.1080/15476286.2020.1809197

Calado, A., Treichel, N., Müller, E. C., Otto, A., & Kutay, U. (2002). Exportin-5-mediated nuclear export of eukaryotic elongation factor 1A and tRNA. *The EMBO journal*, *21*(22), 6216–6224. https://doi.org/10.1093/emboj/cdf620

Chatterjee, K., Majumder, S., Wan, Y., Shah, V., Wu, J., Huang, H. Y., & Hopper, A. K. (2017). Sharing the load: Mex67–Mtr2 cofunctions with Los1 in primary tRNA nuclear export. *Genes and Development*, *31*(21), 2186–2198. https://doi.org/10.1101/gad.305904.117

Chatterjee, K., Nostramo, R. T., Wan, Y., & Hopper, A. K. (2018). tRNA dynamics between the nucleus, cytoplasm and mitochondrial surface: Location, location, location. *Biochimica et Biophysica Acta - Gene Regulatory Mechanisms*, *1861*(4), 373–386. https://doi.org/10.1016/j.bbagrm.2017.11.007

Chomczynski, P., & Sacchi, N. (2006). The single-step method of RNA isolation by acid guanidinium thiocyanate–phenol–chloroform extraction: twenty-something years on. *Nature Protocols*, *1*(2), 581–585. https://doi.org/10.1038/nprot.2006.83

Dultz, E., Wojtynek, M., Medalia, O., & Onischenko, E. (2022). The Nuclear Pore Complex: Birth, Life, and Death of a Cellular Behemoth. *Cells*, *11*(9), 1456. https://doi.org/10.3390/cells11091456

Fenn, K., & Matthews, K. R. (2007). The cell biology of Trypanosoma brucei differentiation. *Current Opinion in Microbiology*, *10*(6), 539–546. https://doi.org/10.1016/j.mib.2007.09.014

Fergus, C., Barnes, D., Alqasem, M. A., & Kelly, V. P. (2015). The queuine micronutrient: Charting a course from microbe to man. *Nutrients*, *7*(4), 2897–2929. https://doi.org/10.3390/nu7042897

Ferguson, M. A. J., Homans, S. W., Dwek, R. A., & Rademacher, T. W. (1988). Glycosyl-Phosphatidylinositol Moiety That Anchors Trypanosoma brucei Variant Surface Glycoprotein to the Membrane. *Science*, 239(4841), 753–759. https://doi.org/10.1126/science.3340856

Fried, H., & Kutay, U. (2003). Nucleocytoplasmic transport: Taking an inventory. *Cellular and Molecular Life Sciences*, *60*(8), 1659–1688. https://doi.org/10.1007/s00018-003-3070-3

Gommers-Ampt, J. H., Van Leeuwen, F., de Beer, A. L., Vliegenthart, J. F., Dizdaroglu, M., Kowalak, J. A., Crain, P. F., & Borst, P. (1993). beta-D-glucosyl-hydroxymethyluracil: a novel modified base present in the DNA of the parasitic protozoan T. brucei. *Cell*, *75*(6), 1129–1136. https://doi.org/10.1016/0092-8674(93)90322-h

Harel, A., & Forbes, D. J. (2004). Importin Beta: Conducting a Much Larger Cellular Symphony. *Molecular Cell*, *16*(3), 319-330. https://doi.org/10.1016/j.molcel.2004.10.026

Hegedűsová, E., Kulkarni, S., Burgman, B., Alfonzo, J. D., & Paris, Z. (2019). The general mRNA exporters Mex67 and Mtr2 play distinct roles in nuclear export of tRNAs in Trypanosoma brucei. *Nucleic Acids Research*, *47*(16), 8620–8631. https://doi.org/10.1093/NAR/GKZ671

Hopper, A. K. (2013). Transfer RNA Post-Transcriptional Processing, Turnover, and Subcellular Dynamics in the Yeast *Saccharomyces cerevisiae*. *Genetics*, *194*(1), 1, 43–67. https://doi.org/10.1534/genetics.112.147470

Hopper, A. K., & Huang, H.Y. (2015). Quality Control Pathways for Nucleus-Encoded Eukaryotic tRNA Biosynthesis and Subcellular Trafficking. *Molecular and Cellular Biology*, *35*(12), 2052-2058. https://doi.org/10.1128/MCB.00131-15

Huang, H. Y., & Hopper, A. K. (2016). Multiple Layers of Stress-Induced Regulation in tRNA Biology. *Life*, *6*(2), 16. https://doi.org/10.3390/LIFE6020016

Huang, H. Y., & Hopper, A. K. (2015). In vivo biochemical analyses reveal distinct roles of β-importins and eEF1A in tRNA subcellular traffic. *Genes & development*, *29*(7), 772–783. https://doi.org/10.1101/gad.258293.115

Hurto, R. L., Tong, A. H. Y., Boone, C., & Hopper, A. K. (2007). Inorganic phosphate deprivation causes tRNA nuclear accumulation via retrograde transport in Saccharomyces cerevisiae. *Genetics*, *176*(2), 841–852. https://doi.org/10.1534/genetics.106.069732

Ibba, M., & Söll, D. (1999). Quality Control Mechanisms During Translation. *Science*, *286*(5446), 1893-1897. https://doi.org/10.1126/science.286.5446.1893

Igloi, G. L., & Kössel, H. (1985). Affinity electrophoresis for monitoring terminal phosphorylation and the presence of queuosine in RNA. Application of polyacrylamide containing a covalently bound boronic acid. *Nucleic Acids Research*, *13*(19), 6881–6898. https://doi.org/10.1093/NAR/13.19.6881

Kessler, A. C., Kulkarni, S. S., Paulines, M. J., Rubio, M. A. T., Limbach, P. A., Paris, Z., & Alfonzo, J. D. (2018). Retrograde nuclear transport from the cytoplasm is required for tRNATyr maturation in T. brucei. *RNA Biology*, *15*(4–5), 528–536. https://doi.org/10.1080/15476286.2017.1377878

Krahn, N., Fischer, J. T., & Söll, D. (2020). Naturally Occurring tRNAs With Non-canonical Structures. *Frontiers in Microbiology*, *11*. https://doi.org/10.3389/fmicb.2020.596914

Kramer, E. B., & Hopper, A. K. (2013). Retrograde transfer RNA nuclear import provides a new level of tRNA quality control in Saccharomyces cerevisiae. *Proceedings of the National Academy of Sciences of the United States of America*, *110*(52), 21042–21047. https://doi.org/10.1073/pnas.1316579110

Li, F. J., & He, C. Y. (2017). Autophagy in protozoan parasites: Trypanosoma brucei as a model. *Future Microbiology*, *12*(15), 1337–1340. https://doi.org/10.2217/fmb-2017-0158

Lukeš, J., Speijer, D., Zíková, A., Alfonzo, J. D., Hashimi, H., & Field, M. C. (2023). Trypanosomes as a magnifying glass for cell and molecular biology. *Trends in Parasitology*, *39*(11), 902–912. https://doi.org/10.1016/J.PT.2023.08.004

Nishimura, S. (1983). Structure, biosynthesis, and function of queuosine in transfer RNA. *Progress in Nucleic Acid Research and Molecular Biology*, *28*, 49-73. https://doi.org/10.1016/S0079-6603(08)60082-3

Nostramo, R. T., & Hopper, A. K. (2020). A novel assay provides insight into tRNAPheretrograde nuclear import and re-export in S. Cerevisiae. *Nucleic Acids Research*, *48*(20), 11577–11588. https://doi.org/10.1093/nar/gkaa879

Ohira, T., & Suzuki, T. (2011). Retrograde nuclear import of tRNA precursors is required for modified base biogenesis in yeast. *Proceedings of the National Academy of Sciences*, *108*(26), 10502-10507. https://doi.org/10.1073/pnas.1105645108

Ooi, C. P., & Bastin, P. (2013). More than meets the eye: Understanding Trypanosoma brucei morphology in the tsetse. *Frontiers in Cellular and Infection Microbiology*, *3*, 1-12. https://doi.org/10.3389/fcimb.2013.00071

Paris, Z. (2021). Nuclear tRNA export in trypanosomes: a journey full of twists and turns guided by tRNA modifications. *Parasitology*, *148*(10), 1219–1222. https://doi.org/10.1017/S0031182021000482

Pemberton, L. F., & Paschal, B. M. (2005). Mechanisms of receptor-mediated nuclear import and nuclear export. *Traffic*, *6*(3), 187–198. https://doi.org/10.1111/j.1600-0854.2005.00270.x

Phizicky, E. M., & Hopper, A. K. (2023). The life and times of a tRNA. *RNA, 29*(7), 898-957. https://doi.org/10.1261/rna.079620.123

Raina, M., & Ibba, M. (2014). tRNAs as regulators of biological processes. *Frontiers in Genetics*, *5*. https://doi.org/10.3389/fgene.2014.00171

Schwenzer, H., Jühling, F., Chu, A., Pallett, L. J., Baumert, T. F., Maini, M., & Fassati, A. (2019). Oxidative Stress Triggers Selective tRNA Retrograde Transport in Human Cells during the Integrated Stress Response. *Cell Reports*, *26*(12), 3416-3428.e5. https://doi.org/10.1016/j.celrep.2019.02.077

Shaheen, H. H., & Hopper, A. K. (2005). Retrograde movement of tRNAs from the cytoplasm to the nucleus in Saccharomyces cerevisiae. *Proceedings of the National Academy of Sciences of the United States of America*, *102*(32), 11290–11295. https://doi.org/10.1073/pnas.0503836102

Whitney, M. L., Hurto, R. L., Shaheen, H. H., & Hopper, A. K. (2007). Rapid and reversible nuclear accumulation of cytoplasmic tRNA in response to nutrient availability. *Molecular Biology of the Cell*, *18*(7), 2678–2686. https://doi.org/10.1091/mbc.E07-01-0006

Wickstead, B., Ersfeld, K., & Gull, K. (2002). Targeting of a tetracycline-inducible expression system to the transcriptionally silent minichromosomes of *Trypanosoma brucei*. *Molecular and Biochemical Parasitology*, *125*(1-2), 211-216. https://doi.org/10.1016/S0166-6851(02)00238-4

Wu, J., Bao, A., Chatterjee, K., Wan, Y., & Hopper, A. K. (2015). Genome-wide screen uncovers novel pathways for tRNA processing and nuclear-cytoplasmic dynamics. *Genes & development*, *29*(24), 2633–2644. https://doi.org/10.1101/gad.269803.115

Yoshihisa, T., Yunoki-Esaki, K., Ohshima, C., Tanaka, N., & Endo, T. (2003). Possibility of cytoplasmic pre-tRNA splicing: The yeast tRNA splicing endonuclease mainly localizes on the mitochondria. *Molecular Biology of the Cell*, *14*(8), 3065–3505. https://doi.org/10.1091/mbc.E02-11-0757

Zhang, W., Foo, M., Eren, A. M., & Pan, T. (2022). tRNA modification dynamics from individual organisms to metaepitranscriptomics of microbiomes. *Molecular Cell* , *82*(5), 891–906. https://doi.org/10.1016/j.molcel.2021.12.007